Available online at www.sciencedirect.com
SCIENCE DIRECT®
Physics and Chemistry of the Earth 29 (2004) 589–598
PHYSICS and CHEMISTRY of the EARTH
www.elsevier.com/locate/pce

Middle latitude LF (40 kHz) phase variations associated with earthquakes for quiet and disturbed geomagnetic conditions

A. Rozhnoi [a,*], M.S. Solovieva [a], O.A. Molchanov [a], M. Hayakawa [b]

[a] *Institute of Physics of the Earth, Russian Academy of Sciences, B. Gruzinskay, 10, Moscow, 123995, Russia*
[b] *Department of Electronic Engineering, The University of Electro-Communications, Tokyo, Japan*

Received 30 May 2003; received in revised form 20 July 2003; accepted 29 July 2003

Abstract

The phase (P) and amplitude (A) anomalies in subionospheric LF signal (40 kHz) along the path Japan–Kamchatka of 2300 km have been studied for the data observed by means of a digital OminiPAL receiver for 2 years. The empirical model of background P and A daily variations for quiet and disturbed geomagnetic conditions in the absence of seismic activity is developed. We pay special attention to the P and A features during large magnetic storms. A sensitivity threshold of LF signal to deforming influence of the geomagnetic and seismic factors is defined. Two cases of bay-like behavior of LF phase and amplitude in nighttime are described as a clear earthquake precursor of LF signal. We have found from the statistical study that LF signal effect is observed only for earthquakes with $M \geqslant 5.5$ and we discuss the possible mechanisms of the effect.

Keywords: VLF/LF anomalies; Earthquakes; Ionospheric perturbations

1. Introduction

VLF/LF subionospheric radio wave monitoring is widely used in recent years for an analysis of earthquake preparatory processes. There are two possible methods for such a study. The first is based on the analysis of nighttime phase anomalies for the long paths. First "bay-like" phase anomalies of Omega signal (10.2–13.6 kHz) were observed on the third and second night before the Gindukush earthquake with $M = 6.7$ (Gokhberg et al., 1989). Similar phase anomalies were detected during 1–16 days before the Rudbar ($M = 7.5$) and the Rachinsk ($M = 7.1$) earthquakes (Gufeld et al., 1992). Intensity variations of Omega signal were found within 1–10 days before strong earthquakes (Morgounov et al., 1994). The second method is terminator time (TT) method, which is based on determination of the characteristic minimums in the phase and amplitude daily variations during sunset and sunrise. This method was applied to the analysis of VLF signals transmitted by an Omega station in Tsushima (Japan) and received at the Inubo receiving observatory (Hayakawa et al., 1996a,b). They found anomalous shift in fluctuations of TT, 3 days before the main shock of the Kobe earthquake ($M = 7.2$). Using this TT method for 11 large seismic events with $M > 6$, Molchanov and Hayakawa (1998) have found that anomalous shift in TT fluctuations appeared in a time interval from 5 to 10 days before large crustal earthquakes and disappeared a few days after them.

It is well known, however, that the phase anomalies of VLF navigation signals are first of all connected with magnetic storms and solar energetic particle fluxes (e.g. Belrose and Thomas, 1968; Kikuchi, 1981; Potemra and Rosenberg, 1973; Sauer et al., 1987). In order to separate the seismic and geomagnetic VLF/LF signal anomalies both of their properties should be established. In this work we examine the nighttime mid-latitude amplitude and phase anomalies of LF signals in order to define a threshold of LF signal sensitivity to deforming influence of the geomagnetic, solar, and seismic factors.

2. Description of measurements

Our receiver is installed in Petropavlovsk–Kamchatka (53° 09′N, 158° 55′E), which measures the phase and amplitude of the LF signals from a radio

* Corresponding author. Tel.: +7-95-254-93-93.
E-mail address: rozhnoi@uipe-ras.scgis.ru (A. Rozhnoi).

1474-7065/$ - see front matter
doi:10.1016/j.pce.2003.08.061

transmitter JG2AS (40 kHz) in Japan (36° 18′N, 139° 85′E). The length of wave path is about 2300 km, and the sampling frequency is 20 sec. We analyze the results of our observations during the period of 2001–2002 using the advanced digital VLF/LF receiver OmniPAL. This receiver can track simultaneously the phase and amplitude of signals from one to five stations. In addition to the Japanese transmitter we receive the signals from transmitters in Australia (19.8 kHz), China (22.2 kHz), and Hawaii (21.4 kHz) for the control.

The location of the transmitter and receiver together with the positions of epicenters of earthquakes ($M \geqslant 4$) for the period 2001–2002 is illustrated in Fig. 1. The area of sensitivity along the wave path with width of 2nd Fresnel zone (~300 km) is also displayed. The area of wave path sensitivity is seen to cover almost completely highly seismically active Izu–Bonin and Kurile–Kamchatka arcs. The epicentral zone can be divided into the different regions which are characterized by distinctly different seismic activity and focal zone depths. Maximal focal depths in this region are 600–650 km, and the upper mantle has a complicated mosaic-layered structure. There are some low velocity zones and the depth of lithosphere is about 60 km.

During the monitoring for 2 years in the area of wave path sensitivity 565 earthquakes with $M \geqslant 4$ and 32 events with $M \geqslant 5.5$ have been registered (according to the Denver catalog). This can be seen from Fig. 1, in which the magnitude of earthquakes is indicated mainly by the symbol size. The maximal earthquake magnitude is 6.8. The distributions of earthquakes as functions of depth and magnitude M are illustrated in the inset of Fig. 1. A high level of seismicity along the LF signal wave path and the complicated structure of the focal zone make it difficult to study the correlation of phase and amplitude variations of LF signal with the seismic events.

3. Data processing

We have made the empirical model of daily distribution of background phase and amplitude variations for each month. Diurnal variations of the amplitude and phase of LF signal changes significantly from month to month. Therefore we use, for our analysis, a residual signal of phase dP or amplitude dA defined as the difference between the observed signal and the average of a few quiet days immediately preceding or following the current day (±5 days):

$$\mathrm{d}A(t) = A(t) - \langle A \rangle, \quad \mathrm{d}P(t) = P(t) - \langle P \rangle,$$

where $A(t)$ and $P(t)$ are the amplitude and phase for the current day, while $\langle A \rangle$ and $\langle P \rangle$ are the corresponding averages. The signal is considered as anomalous when dP or dA exceeds the corresponding standard deviation (σ) as is shown in the lower part of Fig. 2.

Very low frequency and low frequency (VLF/LF) waves are known to be reflected from the lowest region of the ionosphere (the D region during daylight and the lower E region at night), and apart from the sunrise and sunset periods, they exhibit propagation characteristics that are very stable both in phase and amplitude. Therefore, the night and day time periods are chosen for each data with excluding the sunrise and sunset periods as is seen from Fig. 2 (while Hayakawa et al. (1996a,b),

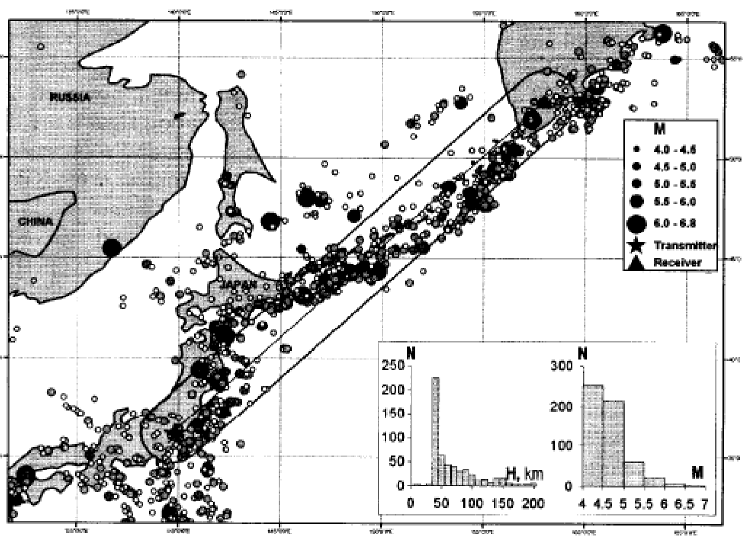

Fig. 1. Location of a radio transmitter and the receiver system together with the EQ ($M \geqslant 4$) epicenters for the period of 2001–2002. The inset illustrates the histograms of EQ distribution versus depth (H) and M. The 1st Fresnel zone is plotted.

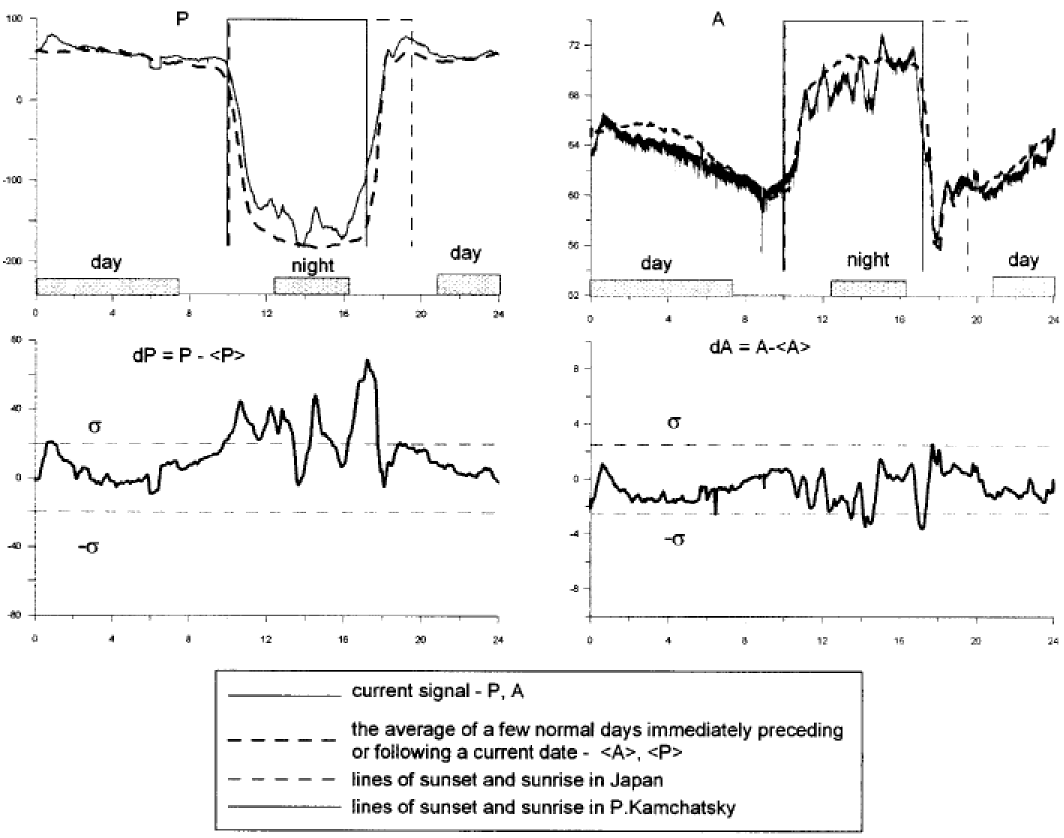

Fig. 2. An example of daily variation of LF signal amplitude and phase (upper two panels). The full lines refer to the current signals (P, A) and the broken lines, the average diurnal variations. Day and night are defined excluding the terminator times. For our reference, the times of sunrise and sunset at the transmitter and receiver are also plotted. The lower two panels indicate dP and dA.

Molchanov et al. (1998) and Molchanov and Hayakawa (1998) have paid special attention to these transition periods). The upper two panels refer to the diurnal variations in phase (left) and amplitude (right). The full lines refer to the current signal, while the broken lines, diurnal average variations. Also, the time periods of days and nights are defined, with avoiding the sunrise and sunset periods. For our reference the time of sunset and sunrise in Japan and in Kamchatsky are indicated as well.

In night and day time periods for each data the averages dP and dA and their dispersions are estimated. Because the daytime variations of LF signals are less than the night ones and they are strongly influenced by sudden ionospheric disturbances (SID) caused by X-rays emitted during a solar flare on the dayside of the Earth, we have chosen only the night conditions for our analysis.

Fig. 3 demonstrates the temporal evolution of daily average dP for nighttime during monitoring of 2 years (top panel) and its spectrum (bottom panel) and wavelet spectrum in the form of contour map (middle panel). Molchanov and Hayakawa (1998) and Hayakawa et al. (2002) have performed this kind of analysis for the terminator times. As can be seen from Fig. 3 we notice the period of 5–45 days in the fluctuations of phase signal. The wavelet analysis of LF signal reveals that there occur fluctuations with period of 5–12 days during the whole observation period of 2 years and longer-period variations are typical only in winter. Quasi-periodic oscillations in VLF propagation parameters have been discovered and discussed in our recent papers on the basis of the TT method (Molchanov and Hayakawa, 1998; Molchanov et al., 2001) and on the basis of d$A(t)$, d$P(t)$ fluctuation analysis (Shvets et al., 2003).

4. Results of analysis

In this paper we study the sensitivity of LF signal amplitude and phase to ionospheric perturbations associated with the variations in magnetic, solar and seismic activity. We use the following parameters: planetary index of magnetic field activity K_p, *Dst*-index, X-rays and electron and proton fluxes (derived from the satellite GOES-10) as well as the data from

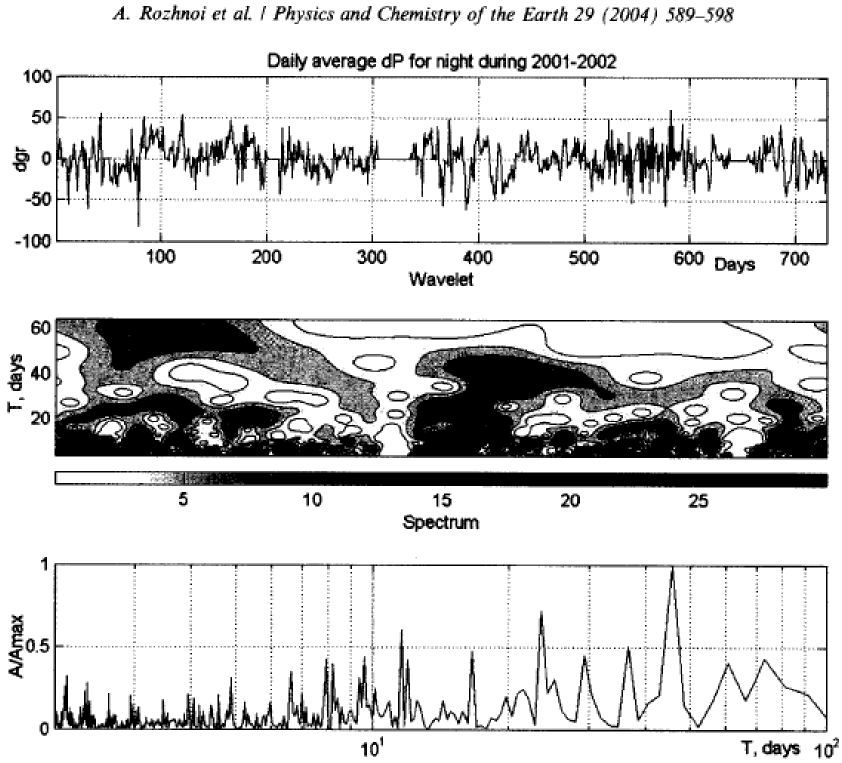

Fig. 3. Temporal evolution of average daily dP nighttime signal for the period 2001–2002 (top). The middle panel illustrates the corresponding result of wavelet analysis. The bottom panel indicates the frequency spectrum.

geomagnetic mid-latitude observatories of Moshiri (MSR, $\Phi = 37.4°$) and Magadan (MGD, $\Phi = 53.6°$) located nearly in the same magnetic meridian as our LF propagation path.

4.1. LF anomalies associated with geomagnetic and solar factors

We use a statistical method to examine the sensitivity of LF signal amplitude and phase to geomagnetic and solar factors. Every parameter analyzed is divided in some intervals with a given value and we estimate the amount of days in which these values are calculated (N). Then in every interval among the chosen days we selected the days on which the average dP or dA or their dispersions exceed their corresponding σ (this will be number of days, N_i. The ratio N_i/N then is considered as sensitivity of LF signal amplitude or phase to the analyzed parameter.

Results of analysis of geomagnetic and solar factors are shown in Fig. 4. Dotted horizontal line indicates the area of random coincidence. As it is seen from the figure (the most left two panels) that the correlation of phase and amplitude variations of LF signal with K_p-index is not found, but there may be a possibility of the moderate tendency to increase for the amplitude variation for larger ΣK_p (greater than 30). The correlation of phase and amplitude variations of LF signal with *Dst*-index is obvious from the 2nd two panels from the left; We have observed a liner correlation for the amplitude with small slope angle since the *Dst* value of 40 nT. As for the phase, the sensitivity is found to begin to increase at 70 nT in |Max*Dst*|, the slope angle is more abrupt and the ratio N_i/N goes to 100% beginning from 120 nT.

Phase and amplitude anomalies and high-pitch-angle-particle fluxes (electrons and protons) registered on the geostationary GOES-10 satellite are found to correlate clearly with each other in Fig. 4 (right two panels). For the proton analysis we choose a channel P1 (0.6–4.2 MeV) and for the electron analysis—a channel E1 (>2 MeV). There is no sensitivity threshold to the particle fluxes both for the amplitude and phase variations. The ratio N_i/N increases up to 100% at 800 particles/(cm^2 s sr) for the electrons and at 300 ions/(cm^2 s sr)/ MeV for the protons.

VLF phase anomalies are typical for the main and recovery phase of magnetic storms. It was found that "bay-like" LF phase and amplitude anomalies are observed during the bursts of Pi3 geomagnetic pulsations at nighttime (sometimes with delay of a few tens of minutes) (Rozhnoi et al., 2002). At the same time the intensity of LF signal variations does not depend linearly on the strength of magnetic storm or substorm. For example, the strong magnetic storm on March 31, 2001 ($Dst = 360$ nT) is accompanied by a small positive phase anomaly. However, a rather modest geomagnetic dis-

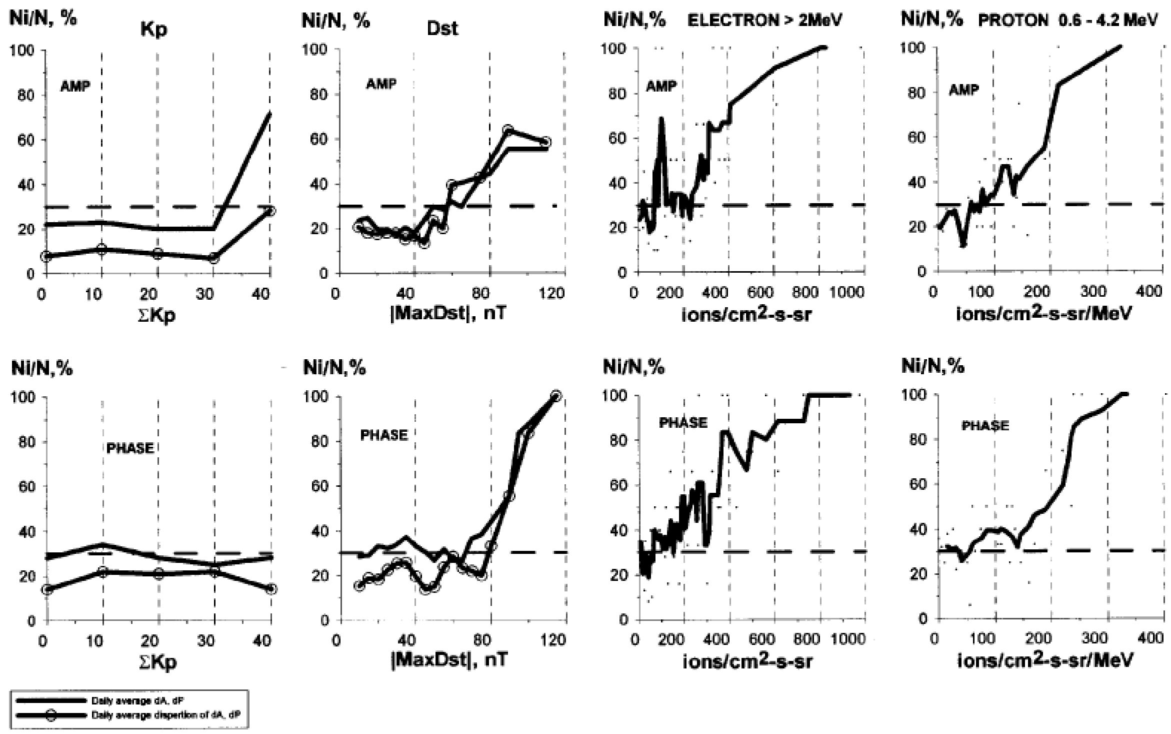

Fig. 4. Dependence of amplitude and phase anomaly on the diurnal ΣK_p and $|\text{Max}Dst|$ indices and on the diurnal average particle fluxes—electron and proton (GOES-10) during 2001–2002. N—number of days in the interval of K_p, Dst or particles. N_i—number of days in the same interval with the data exceeding the corresponding standard deviation (σ).

turbance on January 21, 2001 ($Dst = 40$ nT) has caused a large negative phase anomaly.

Let us consider the strong ($Dst = 250$ nT) magnetic substorm on April 11, 2001. Variations of the amplitude and phase (left upper two panels) simultaneously with magnetograms (X-component) of the observatories Magadan and Moshiri (left lower two panels) and the corresponding dynamic spectra of the signals (right panels) are shown in Fig. 5. For the calculation of dynamic spectrum of amplitude and phase we use the signal filtered in the frequency band of $f = 0.5$–5.0 mHz. It is evident that the development of a substorm on the magnetic meridian of LF wave path is accompanied by the simultaneous negative phase and amplitude anomaly. The dynamic spectra of LF phase and amplitude anomalies have shown the frequency–time wave structure very similar to that of the simultaneously observed Pi3 geomagnetic pulsations ($f = 0.5$–3.0 mHz) from the comparison between the right upper two and right lower two panels in Fig. 5. Thus the behavior of LF signal is determined in many respects by the geomagnetic disturbance and solar activity.

4.2. LF anomalies associated with earthquakes

There are two possibilities to discover the LF anomalies caused by seismic activity. The first method is to select a concrete seismic event and to examine some temporal vicinity around this event with a special purpose to find LF signal anomalies. This tool is mainly applied to strong and isolated seismic shocks. A precursory effect is valid if an anomaly is observed a few days (usually in nighttime) before the event.

The second method is examining the time series in order to find out any statistical interconnection between the seismicity and LF anomalies. We, here, analyze the data series of earthquakes from the Denver's catalog and the data series of the daily average night phase or amplitude and its dispersion.

The examples by the first method in our work include two cases, which are found to show very clearly an abnormal behavior of LF signal before the isolated earthquakes during quiet magnetic conditions. Any anomaly is not registered on the control wave paths of LF signal at this time.

A change in the phase level in nighttime before an earthquake on February 14, 2001(23:36 LT)($M = 5.8$, depth $H = 146$ km, distance from the propagation path $(L) = 3$ km) is demonstrated in Fig. 6. On the left of Fig. 6, we can find the temporal evolutions during the period of Feburary 7–15, 2001 of K_p, X-ray, Dst, earthquake (magnitude, M) (top four panels), dA, A, dP, P (middle four panels), electrons, protons, magnetic records (X-component) at Moshiri (MSR) and Magadan (MGD)

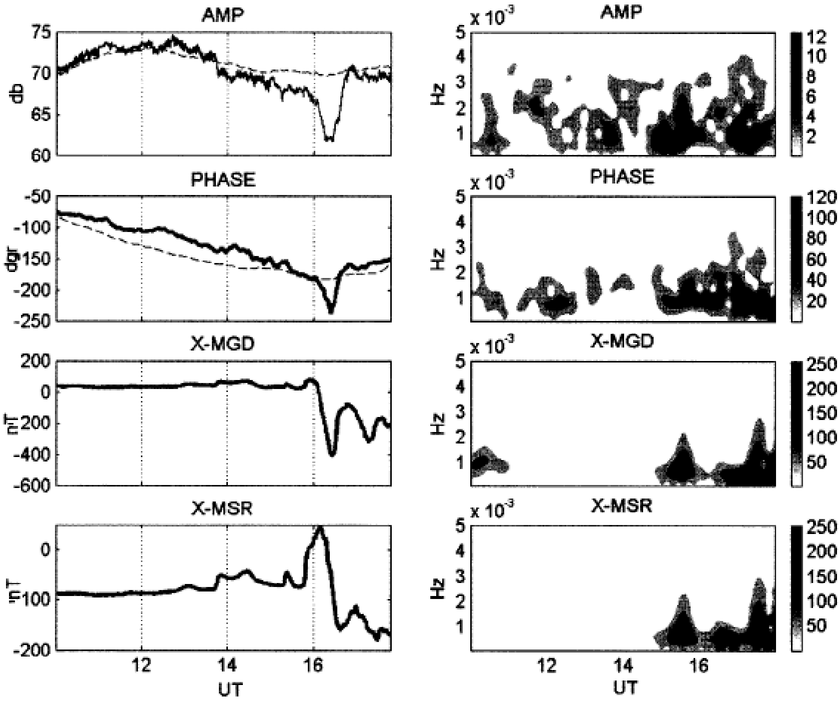

Fig. 5. Phase and amplitude anomalies (left top two panels) and the magnetograms from the observatories Magadan (MGD) and Moshiri (MSR) (left bottom two panels) during a magnetic substorm on April 11, 2001 ($Dst = 250$ nT; $AE = 2300$ nT) and the dynamic spectra of the signals. Dotted line- average of phase and amplitude.

(bottom four panels). Anomalies in the phase are indicated by shading. The right panels illustrate the sequence of daily variation in phase. The shading means the deviation from the average. We can see from the figure that 6 days before the event the signal nighttime level begins to rise sharply, and 2 days before the earthquake the anomaly exceeds σ by more than 2.5 times. The negative anomaly day before the earthquake is probably connected with the development of a substorm which is evidence from the corresponding magnetic field registration at the observatory of Moshiri and from *Dst*-index. Anomalies of LF signal amplitude during the considered period are not observed.

The appearance of a "bay-like" anomaly of LF signal amplitude and phase before an earthquake on March 17, 2001 (17:24 LT), ($M = 5.5$, $H = 103$ km, $L = 8$ km) is shown in Fig. 7. The presentation is the same as in Fig. 6. We can clearly trace the development of a night anomaly both on the signal phase and amplitude 7 days before the earthquake in this example. First 2 days are characterized by significant negative anomaly both on the phase and amplitude of LF signal. Next 3 days the phase anomaly becomes positive in the first half of night and negative in the second half. The phase anomaly in this time exceeds σ-level by more than three times. Last 2 days before the earthquake the phase anomaly is found to become negative again and less. While, the amplitude anomaly is seen to remain negative during all the time interval as seen from the right sequence of A in Fig. 7. It should be noted that before the earthquake on March 17, 2001 in addition to the long-period "bay-like" anomaly of LF signal we have observed a change in frequency of amplitude and phase.

Fig. 8 illustrates the LF signal phase and amplitude and their frequency spectra and wavelets for March 15, 2001. Only nighttime of the signal filtered in a frequency band of 0.5–5.0 mHz (as shown in the second panels) is used for our spectral analysis. The signal maximum with the period 0.5 and 0.9 mHz (30 and 20 min) is clearly observed in the bottom panels. The similar frequency maxima are typical for 3 days before the earthquake when the phase anomaly is positive.

The results of statistical analysis for 2 years of observations are summarized in Fig. 9. The average residual amplitude and phase of the signal (upper two panels in Fig. 9) and their dispersion (bottom two panel) during nighttime are examined during 10 days before and 10 days after an earthquake. Magnitude (M) is divided into four intervals: 4.0–4.5, 4.5–5.0, 5.0–5.5 and 5.5–6.0. In the graph is shown the bar chart where each range is divided into 21 parts (±10 days and day of earthquake), The top of bar chart is the amount of events in the given interval of magnitudes (N), and the bottom of bar chart is the amount of days in which a

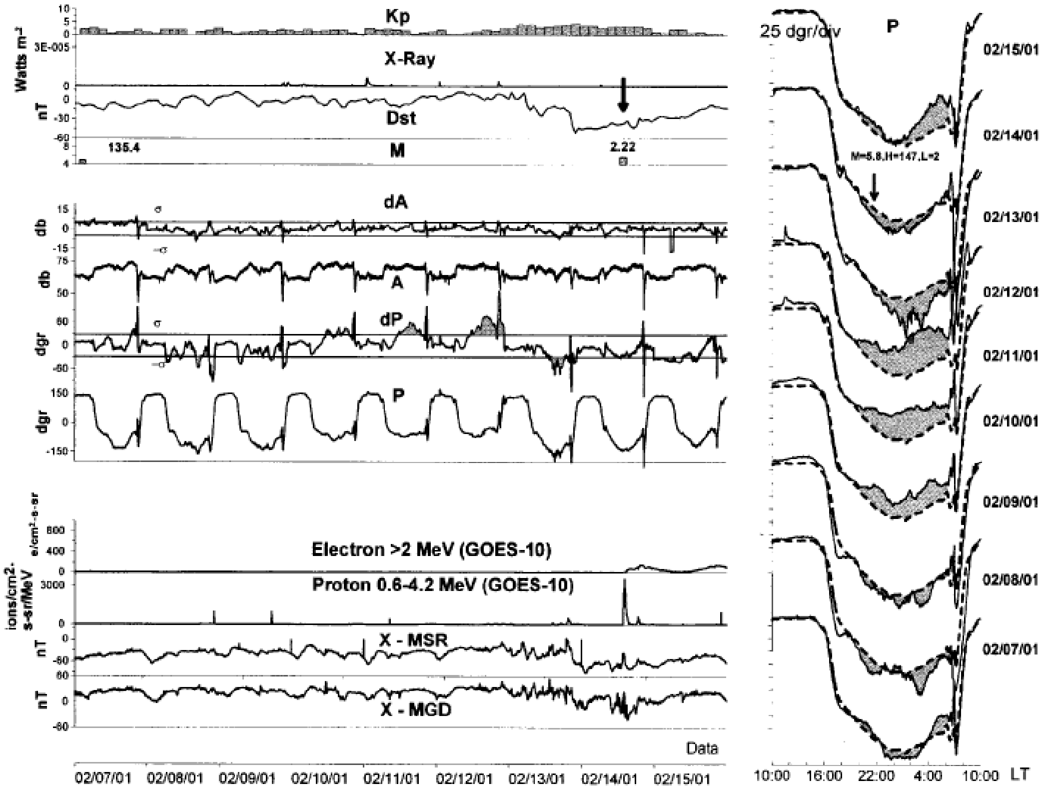

Fig. 6. Charge of phase before an earthquake on February 14, 2001 ($M = 5.8$, $H = 147$ km, $L = 2$ km). Left panels are the records of amplitude (A), phase (P) and its residuals (dA and dP) for the Japan-Kamchatka wave path together with M, K_p and Dst indices, X-ray, electrons, protons, and magnetic field variations at the observatories Magadan (MGD) and Moshiri (MSR) during 7–15 February, 2001. An arrow indicates the time of earthquake. Right panels are the record of phase during 7–15 February, 2001 in which the dotted line is the average phase for quiet days.

signal or its dispersion exceeds the respective σ (N_i). The line is the ratio of N_i/N in percentage and the dotted line is the averaged 2σ level. We can see from the figure that there is no correlation of LF signal anomalies with earthquakes with $M < 5.5$ and with the number of days with regard to the moment of an earthquake. However, when the earthquake magnitude is more enhanced, $5.5 < M < 6$, for the all days the ratio of N_i/N is found to exceed obviously the averaged values by more than 2σ. Thus, on the wave path under the consideration the sensitivity of LF signals (both phase and amplitude and their dispersions) to seismic processes becomes apparent mainly for $M > 5.5$. The most probable times of phase and amplitude anomalies are 7 and 2–3 days before the earthquake and also 6–7 days after it.

5. Discussion and conclusions

The theory of atmosphere–ionosphere boundary layer disturbances caused by seismic activity is not well understood at present (Molchanov et al., 2001), but currently the search for the mechanisms of seismo-ionospheric coupling is carried out in the following three directions: (1) modification of the electric fields and currents in the Earth–ionosphere electric circuit over the earthquake zone, (2) seismic impact on the thunderstorm clouds and (3) transfer of the disturbances from a seismic source to the ionosphere by acoustic and internal gravity waves. It is highly probable that the effect observed is connected with an increase of plasma density perturbations inside the ionosphere, which are induced by preseismic water and gas release on the ground surface and the following energy transportation into the ionosphere by atmospheric gravity waves (Molchanov and Hayakawa, 1998; Molchanov et al., 2001).

In conclusion, we notice the main results of the present work.

- The correlation of phase and amplitude variations of LF signal with K_p-index is not found.
- The correlation of phase and amplitude variations of LF signal with Dst-index, outer-zone particles (protons and electrons) with high-pitch angle is established.
- It was found that LF anomalies are typical for the main phase of a magnetic storm. The similarity of the structure of LF phase and amplitude anomalies

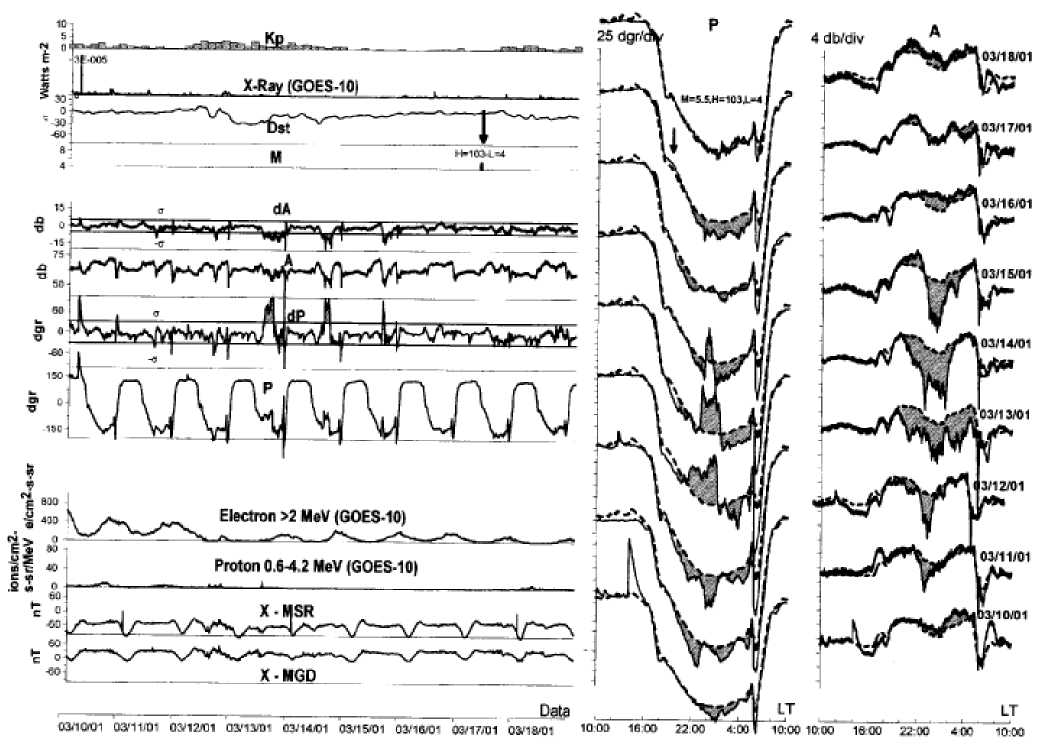

Fig. 7. The same as Fig. 6, but for the earthquake on March 17, 2001 ($M = 5.5$, $H = 103$ km, $L = 4$ km).

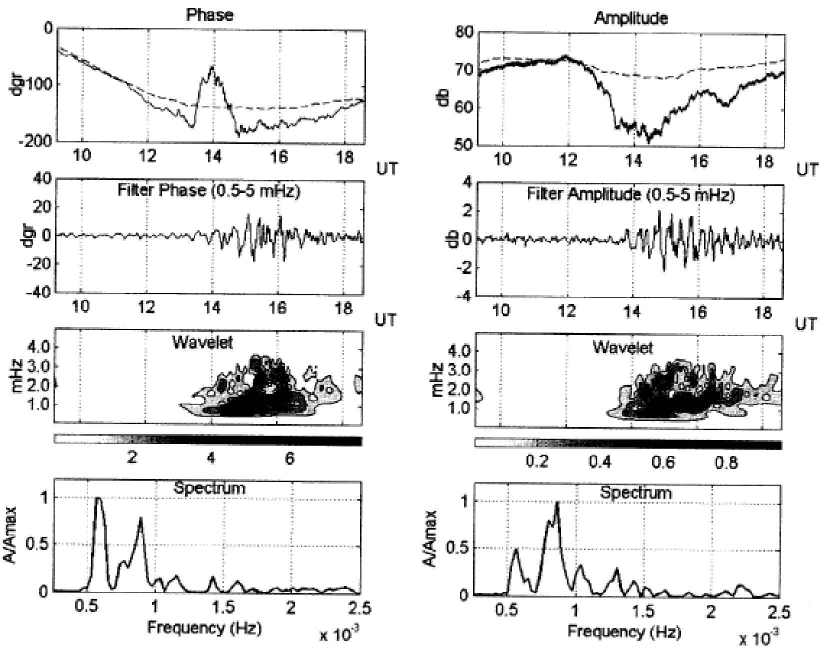

Fig. 8. Phase and amplitude anomalies (top two panels) and their spectra and wavelets (bottom two panels on the left and right) for the filtered signals (second panels on the left and right) for March 15, 2001.

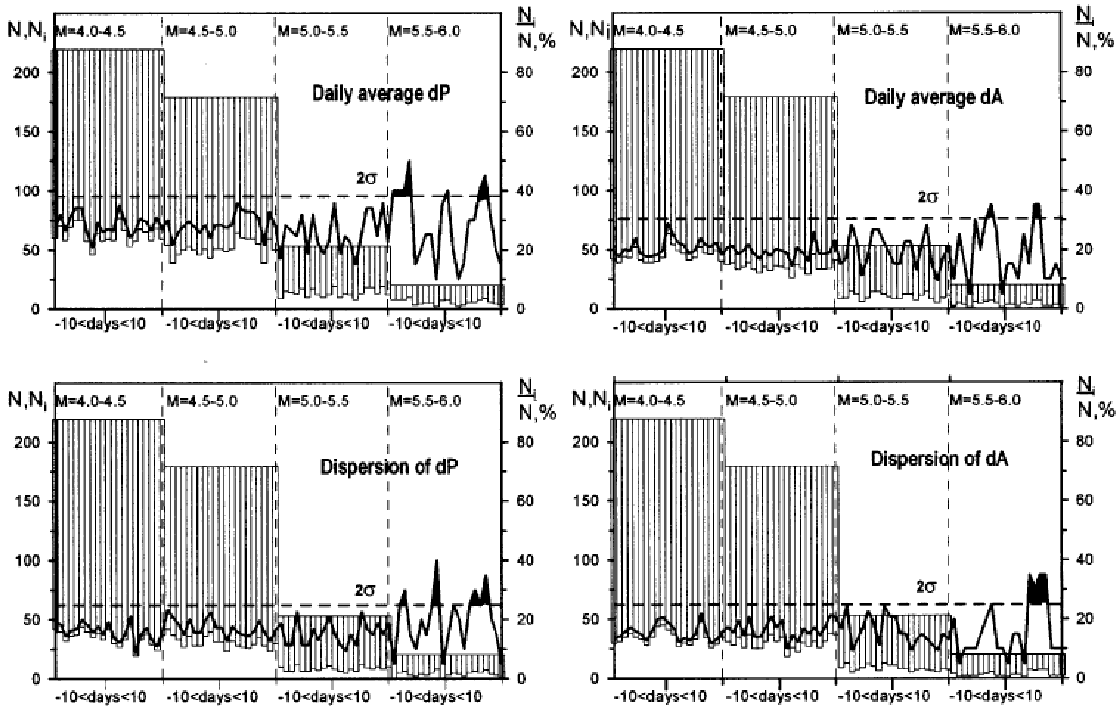

Fig. 9. Dependence of amplitude and phase anomaly on earthquake magnitude during 2001–2002 for the period from 10 days before to 10 days after the earthquake time. Top of the float bar is the number of days in the interval of M (N). Bottom of the float bar is the number of days in the same interval with data exceeding σ (N_i). Solid line is N_i/N, and dotted line is the average of $N_i/N+2\sigma$.

to the structure of the simultaneously observed Pi3 geomagnetic pulsation is found.

- The analysis of phase in nighttime for 2 years has shown that it is subject to the oscillations with period of 5–45 days.
- The connection between anomalies of LF signal in nighttime and earthquakes with $M \geqslant 5.5$ is established.
- The phase and amplitude anomalies of seismic nature and its dispersions well correlate with each other.
- The most probable times of phase and amplitude anomalies 7 and 2–3 days before an earthquake and 6–7 days after it.
- A probable source of atmospheric disturbance of seismic nature could be gravity waves caused by geochemical factors.

Acknowledgements

This research was partially supported by ISTC under Grant 1121 and by Commission of the EU (grant No INTAS01-0456). Two of the authors (O.A.M. and M.H.) are thankful to International Space Science Institute (ISSI) at Bern, Switzerland for their support within the project "Earthquake influence of the ionosphere as evident from satellite density-electric field data". Two Authors (A.A.R and M.S.S.) are grateful to Russian Fund for Basic Research for the grant 02-05-64069, and finally one of the authors (M.H.) is grateful to International Communication Foundation and the Mitsubishi Foundation for their support.

References

Belrose, J.S., Thomas, L., 1968. Ionization in the middle latitude D-region associated with geomagnetic storms. J. Atmos. Terr. Phys. 30, 1397–1413.

Gokhberg, M.B., Gufeld, I.L., Rozhnoi, A.A., Marenko, V.F., Yampolshy, V.S., Ponomarev, E.A., 1989. Study of seismic influence on the ionosphere by super long wave proding of the Earth–ionosphere waveguide. Phy. Earth Planet. Inter. 57, 64–67.

Gufeld, I.L., Rozhnoi, A.A., Tyumensev, S.N., Sherstuk, S.V., Yampolsky, V.S., 1992. Radiowave disturbances in period to Rudber and Rachinsk earthquakes. Phys. Solid Earth 28 (3), 267–270.

Hayakawa, M., Molchanov, O.A., Ondoh, T., Kawai, E., 1996a. Precursory signature of the Kobe earthquake on VLF subionospheric signal. J. Atmos. Electr. 16 (3), 247–257.

Hayakawa, M., Molchanov, O.A., Ondoh, T., Kawai, E., 1996b. Anomalies in subionospheric VLF signal for the 1995 Hyogo-ken Nanbu earthquake. J. Phys. Earth 44, 413–418.

Hayakawa, M., Molchanov, O.A., Shima, N., Shvets, A.V., Yamamoto, N., 2002. Wavelet analysis of disturbances in subionospheric

VLF propagation correlated with earthquakes. In: Hayakawa, M., Molchanov, O.A. (Eds.), Seismo Electromagnetic: Lithosphere–Atmosphere–Ionosphere Coupling. TERRAPUB, Tokyo, pp. 223–228.

Kikuchi, T., 1981. VLF phase anomalies associated with substorm. Mem. Nat. Inst. Polar Res. Special Issue, No. 18, 3–23.

Molchanov, O.A., Hayakawa, M., 1998. Subionospheric VLF signal perturbations possibly related to earthquakes. J. Geophys. Res. 103, 17489–17504.

Molchanov, O.A., Hayakawa, M., Ondoh, T., Kawai, E., 1998. Precursory effects in the subionospheric VLF signals for the Kobe earthquake. Phys. Earth Planet. Inter. 105, 239–248.

Molchanov, O.A., Hayakawa, M., Miyaki, K., 2001. VLF/LF sounding of the lower ionosphere to study the role of atmospheric oscillations in the lithosphere–ionosphere coupling. Adv. Polar Upper Atmos. Res. 15, 146–158.

Morgounov, V.A., Ondoh, T., Nagai, S., 1994. Anomalous variation of VLF signal associated with strong earthquakes ($M \geqslant 7$). In: Hayakawa, M., Fujinawa, Y. (Eds.), Electromagnetic Phenomena Related to Earthquake Prediction. Terra Sci. Pub. Com, Tokyo, pp. 409–415.

Potemra, T.A., Rosenberg, T.J., 1973. VLF propagation disturbances and electron precipitation at mid-latitudes. J. Geophys. Res. 78, 1572–1580.

Rozhnoi, A.A., Kleimenova, N.G., Kozyreva, O.V., Soloviea, M.S., 2002. Storm-time mid-latitude VLF (40 kHz) signal variations. Proceedings of the Fourth International Conference "Problems of Geocosmos". St. Petersburg State University, pp. 204–208.

Sauer, H.H., Spjeldvik, W.N., Steel, F.K., 1987. Relationship between long-term phase advances in high-latitude VLF wave propagation and solar energetic fluxes. Radio Sci. 22, 405–424.